EUROPEAN ORGANIZATION FOR NUCLEAR RESEARCH

CERN-EP/83-86
June 29th, 1983

EXPERIMENTAL J/ψ HADRONIC PRODUCTION FROM 150 TO 280 GeV/c

NA3 COLLABORATION

J. Badier[4], J. Boucrot[5], J. Bourotte[4], G. Burgun[1], O. Callot[5], Ph. Charpentier[1], M. Crozon[3], D.Decamp[5], P. Delpierre[3], B. Gandois[1], R. Hagelberg[2], M. Hansroul[2], Y. Karyotakis[4], W. Kienzle[2], P. Le Dû[1], J. Lefrançois[5], Th. Leray[3a], J. Maillard[3], A. Michelini[2], Ph. Miné[4], G. Rahal[1b], O. Runolfsson[2], P. Siegrist[1], A. Tilquin[3], J. Timmermans[2c], J. Valentin[3], S. Weisz[4].

CEN, Saclay[1]-CERN, Geneva[2]-Collège de France, Paris[3]-
Ecole Polytechnique, Palaiseau[4]-Laboratoire de l'Accélérateur Linéaire, Orsay[5].

ABSTRACT

A detailed study of J/ψ hadronic production has been performed in a high statistics experiment (more than 1.5 10^6 J/ψ observed in their dimuon decay mode). Data have been taken with incident $\pi^{\pm}$, $K^{\pm}$, $p^{\pm}$, on hydrogen and platinum targets, at 150, 200 and 280 GeV/c. We find from the observed nuclear dependance of the cross sections, that about 18% of the J/ψ are produced diffractively. Using known structure functions of the quarks in the nucleon and in the pion, we derive estimations for the gluon structure functions.

a) now at "Agence Française pour la maîtrise de l'Energie", Paris
b) now at CERN, Geneva
c) now at NIKHEF, Amsterdam

Submitted to Zeitschrift für Physik C

1) INTRODUCTION

Since the discovery of the J/ψ meson in 1974 [1], a considerable work has been done to study the hadronic production of this particle. Extensive data have been recorded for incoming protons, from threshold up to highest ISR energies. Data are less abundant for other incident hadrons, in particular at high energies for kaons or antiprotons, which can provide enlightments on the J/ψ production mechanism.

We present in this paper high statistics data (more 1.5 10^6 events) obtained in a beam dump experiment at CERN, from incident identified protons, antiprotons, pions and kaons at 150, 200 and 280 GeV/c.

2) EXPERIMENTAL SET-UP

The J/ψ events analyzed in this paper have been observed in the $\mu^+\mu^-$ decay channel, using the NA3 spectrometer in the "beam dump" configuration. This set-up has been extensively described elsewhere [2]. It was optimized for the study of high mass ($M_{\mu\mu} > 4$ GeV/c^2) Drell-Yan events, but allowed the observation of J/ψ events with a fairly good acceptance, around 25%. We insist in the following only on the points which are relevant for the present J/ψ studies.

2.1 Beam

The data have been taken with an unseparated secondary beam in the CERN SPS North Area; the particles are identified up to 200 GeV/c by two differential Cerenkov counters (CEDAR) and two threshold Cerenkovs. The various beam conditions are summarized in Table 1.

2.2 Targets and dump

Two targets have been used simultaneously : a liquid hydrogen target (50 cm long at 280 GeV/c, 30 cm long at other energies) and a platinum target (6 cm long). The geometrical separation of these targets (about 40 cm from the end of H_2 to the beginning of Pt), and the informations from an interaction counter located downstream the H_2 target, allowed a satisfactory off-line separation of the targets at the J/ψ mass.

The experiment used a hadron absorber, made of stainless steel with a central conical tungsten plug to dump the beam. The length (150 cm) was sufficient to avoid important punch-through; it was located 40 cm downstream the Pt target to allow a good target-dump separation of events without introducing too many pion decays. In the following, events assigned to the dump will never be considered, to avoid problems coming from the reinteraction of secondary particles in the heavy material.

2.3 The spectrometer

It consists of a superconducting magnet giving a dipolar field with 4.1 T.m. of bending power, and 38 MWPC planes which size varies from 1 to 25 m^2. Two configurations of chambers were used, one giving the highest possible acceptance (at 150 and 200 GeV/c) and the other a lower acceptance but a better momentum resolution ($\Delta p/p \sim 2.10^{-4}$ p, p in GeV/c, used at 280 GeV). The muons were identified in a hodoscope located behind a 1.8 m thick iron filter.

2.4 The trigger

The trigger was essentially a condition on P_{Tv}, the vertical component of the transverse momentum. Either two muons with $P_{Tv} > 0.6$ GeV/c, or one with $P_{Tv} > 1$ GeV/c, were required : this eliminates a large fraction of π and K decays.

About 25 10^6 triggers have been registered on tape at the 3 energies considered here.

3) DATA AND ACCEPTANCE

3.1 Cuts on data

After processing through the pattern recognition program, several cuts are performed in order to eliminate background events :

- definition of a fiducial volume inside the detectors
- elimination of dimuons with momentum greater than the beam, taking into account the momentum resolution
- elimination of events with excentric vertex, or with an ambiguous target assignation. The longitudinal resolution on the vertex being around 12 cm, a fraction of J/ψ events are lost because they are assigned by

the reconstruction program to a wrong target; from simulations we estimate this loss to be less than 2%.

- all dimuons with $x_F < 0$ are eliminated, since below this value the acceptance drops rapidly and the reinteraction effects in the Pt target become important.

3.2 Definition of J/ψ events

The mass resolution around the J/ψ mass is about 4% at 150 and 200 GeV/c and 2.5% at 280 GeV/c and comes mainly from the multiple scattering of the muons in the hadron filter. This gives a broad peak for J/ψ candidates, around the mass $M_\psi = 3097$ MeV/c² (Fig. 1). The "J/ψ" events in the following analysis are defined as dimuons with a $\mu^+\mu^-$ topology and a mass $M_{\mu\mu}$:

$$2.7 \text{ GeV/c}^2 < M_{\mu\mu} < 3.5 \text{ GeV/c}^2$$

In this mass interval the contamination from π and K decays may be estimated from like-sign dimuons and is found negligible (< 0.5%). The main contamination comes from continuum events and is estimated around 7% at all energies, from an interpolation of the data between 4.1 - 4.5 GeV/c² and 2.0 - 2.4 GeV/c². In the following all numbers and experimental distributions concerning J/ψ's will be given after subtraction of this background, the interpolation being made in each bin.

In Table 2 we give the number of events obtained in the various conditions with the two targets. The statistics is quite large and thus most of the results given in this paper will be dominated by systematic errors rather than by statistical errors.

3.3 Acceptance

The acceptance of the apparatus has been computed using a Monte Carlo program which takes into account all known efficiencies of the detector, trigger effects and cuts. Special care has been taken to simulate properly the beam dump and the detailed behaviour of the triggering device. The simulated events are then processed by the same chain of programs as real events.

The events are generated according to the observed x_F and P_T distributions, following an iterative procedure. The decay of the J/ψ is assumed to be isotropic, although the λ parameter of the angular distribution was found to be non-zero (section 10). However, our $\cos\theta$-acceptance is restricted around $\cos\theta = 0$ and a change in λ does not affect this region. Thus the acceptance integrated over $\cos\theta$ is not very sensitive to the value of λ used in the simulation.

The various uncertainties which remain in the simulation as well as the effect of $\lambda = 0$ may contribute to a systematic error around 3% in the results on integrated quantities and of about 5 to 10% on the differential distributions.

4) EXPERIMENTAL AND THEORETICAL SITUATION

4.1 Previous results on J/ψ production by pions

Results on J/ψ production by π meson beams have already been published. In the low energy range, two Serpukhov experiments have used 27 to 70 GeV/c beams, studying mainly the A dependence [3] and the production cross section [4]. An experiment performed at the Ω spectrometer has produced a very extensive study of J/ψ production by $\pi^{\pm}$, $K^{\pm}$, $p^{\pm}$ beams at 39.5 GeV/c. It has for the first time shown that J/ψ are produced by pions mainly in the forward direction [5], and compared the production yields for various incident particle on two different targets (H_2 and tungsten) [6]. They have also confirmed our discovery of a strange effect [7] in the x_F behaviour of the A-dependence [8].

At higher energy, the WA11 experiment at CERN has studied in an open geometry spectrometer the J/ψ production by 150 and 190 GeV π^- [9]. The study of the associated photons allowed them to measure the yield of J/ψ production through χ states [10]. They estimated the gluon structure function in the pion using the differential cross-section $d\sigma/dx$ of their 50 000 J/ψ produced on beryllium [11].

The CIP collaboration has studied J/ψ production by various beams at 225 GeV/c, studying cross-sections [12] and the A-dependence [13]. New results have been provided by the E-537 experiment at FNAL on J/ψ production by pions and antiprotons at 125 GeV/c [14].

4.2 ψ - nucleon total cross section from photoproduction

A large number of experiments have reported on J/ψ production by photons (real and virtual). These results have been interpreted in the frame of the vector dominance model which connect the vector meson production cross section to its total interaction cross section. This model gave very interesting results already for ρ-N, ω-N and φ-N cross sections.

The most recent result from the EMC collaboration [15] gives the following values :

$\sigma(\psi N \to \psi + X) = 79 \pm 12$ μb

$\psi_{tot}(\psi N) = 2.2 \pm 0.7$ mb

Previous experiments [16] showed that the ψ-N total cross section increases rapidly at the $D\bar{D}$ production threshold, showing that the observed cross section is mainly due to $\psi N \to D\bar{D} + X$. The same value was obtained from the A-dependence of the J/ψ photoproduction [16] :

$\sigma_{abs}(\psi N) = 2.75 \pm 0.90$ mb

In conclusion, one has strong evidence that the ψ-nucleon total cross section is small and that the quasi-elastic cross section is, as expected [17] negligible.

4.3 Models for J/ψ hadronic production

Our intent is not to review all the available litterature about this subject, as it was already done by R.J.N. Phillips [18].

The main idea is that J/ψ production proceeds mainly through light quark and gluon fusion. Charmed-quark fusion is not favoured by the experimental yield of $\psi D\bar{D}$ associated production.

Detailed calculations of $c\bar{c}$ pair production by both $q\bar{q}$ and gg mechanism have been made, which explain reasonably well the evolution of the cross section with incoming energy as well as the shape of the differential cross-section [19]. The fact that the absolute cross section is not prescribed by the models allows for other production sources to be present, as was suggested by Teper [20] or even from the intrinsic charm component of the incoming hadron [21].

5) NUCLEAR EFFECTS IN J/ψ PRODUCTION

5.1 Dependance of cross sections with A (atomic number of the target)

The nuclear dependance of cross sections is usually parametrized as

$$\sigma(\text{A-nucleus}) = A^{\alpha}\ \sigma_0 \qquad (5.1)$$

Since we have data on platinum nuclei (A = 195.09 with Z/A = 0.4) and on hydrogen, we can derive the values of the exponent α for different incident particles. We have to take into account the neutron/proton proportions in the Platinum nucleus. Using the following relation (from isospin invariance) :

$$\sigma(\pi^+ p \to \psi + X) = \sigma(\pi^- n \to \psi + X) \qquad (5.2)$$

we may write :

$$\begin{aligned} \sigma(\pi^- Pt \to \psi + X) &= A^{\alpha}[0.6\sigma^+ + 0.4\sigma^-] \\ \sigma(\pi^+ Pt \to \psi + X) &= A^{\alpha}[0.6\sigma^- + 0.4\sigma^+] \end{aligned} \qquad (5.3)$$

if $\sigma^- = \sigma(\pi^- p \to \psi + X)$ and $\sigma^+ = \sigma(\pi^+ p \to \psi + X)$

The ratio σ^+/σ^- is measured (see section 6) to be 0.92 ± 0.03 at 200 GeV/c and 0.95 ± 0.03 at 150 GeV/c, and thus the correction due to the nucleon content of the targets is less than 5%.

We deduce the values of α listed in Table 3 for incident π^+, p and π^-. They can be summarized as follows :

$\alpha = 0.96 \pm 0.01$ for pions

$\alpha = 0.94 \pm 0.03$ for protons

These values are significantly different from 1., which would be expected if the J/ψ production mechanism were purely a fusion of constituent partons as in the Drell-Yan mechanism [22] and if the J/ψ could not interact inside the nucleus. They are also very far from the value (around 0.7) which is found in inclusive production of low mass hadrons. We have thus to go into a detailed study of these nuclear effects as a function of kinematical variables, in order to obtain indications on the J/ψ production mechanism.

5.2 H_2/Pt cross sections : variations with x_F and P_T

We will consider the ratio of the cross sections on hydrogen and platinum :

$R = A\sigma(H_2)/\sigma(Pt)$

This ratio is related to the usual exponent α through the formula $R = A^{1-\alpha}$. This quantity is free of flux normalization errors : the results depend only on the knowledge of the relative acceptances, and of the effective numbers of nucleons. R has been studied as a function of the kinematical variables x_F and p_T.

We give in Fig. 2 to 4 the results for $R(x_F)$, $R(P_T)$, and $R(x_F)$ for slices of P_T. Qualitatively, $R(x_F)$ increases strongly as $x_F \to 1$, which is very different from the flat behaviour of the same quantity in Drell-Yan events. The $R(P_T)$ behaviour is also surprising, since it decreases strongly when P_T increases. Let us recall that this behaviour was also observed in the Ω experiment [8], and also some indication appeared in ref. [3], although it was not claimed at all, but their value of α dropped from 0.97 at $x_F = 0$ to 0.7 at $x_F = 1$.

These results are not easy to explain. The behaviour of $R(x_F)$ and $R(P_T)$ differs strongly from what occurs in a pure parton fusion mechanism such as the Drell-Yan. This means that interactions either in the initial state (diffusion of the π or p in the heavy nucleus) or in the final state (ψ - nucleon diffusion) are at work : this has to be studied quantitatively.

5.3 Evidence for a new production mechanism of the J/ψ

We shall see in the following that the observed behaviour of $R(x_F)$ and $R(P_T)$ cannot be explained if the J/ψ is only produced through parton fusion, even if we consider that the J/ψ can reinteract inside the nucleus. This will lead us to consider that a fraction of the J/ψ's are produced through another mechanism.

In the framework of a parton fusion mechanism, only final state ψ-nucleon reinteractions can modify $R(x_F)$ and $R(P_T)$. The space-time extension of the interaction is not so well known, but one can estimate that the life-time of the intermediate virtual state leading to the observed J/ψ is of the order of h/M, where M is its mass. This means (see ref. [23] for details), that the J/ψ's are produced very close from the interaction point at $x_F = 0$, and that almost one half is produced outside the nucleus at $x_F = 1$. The expected behaviour of $R(x_F)$ is then a decrease from about 1.2 (corresponding to a ψ-nucleon absorption cross section of 2mb) towards a value closer from 1. However, one could imagine, ignoring the photoproduction results, that the J/ψ interacts very inelastically before leaving the nucleus. The observed effect would correspond to a cross-section $\psi N \rightarrow \psi + X$ of more than 12 mb (value obtained assuming that at $x_F = 1$, the ψ is produced at the interaction point). This value is in contradiction with all expected or measured [15, 16] ψ-nucleon cross sections (see section 4.2). The observed behaviour at $x_F = 0$ ($R(x_F = 0) \simeq 1.2$) is in good agreement with these expectations of parton fusion, whereas when x_F increases, $R(x_F)$ does not follow the expected trend.

At large x_F, the only explanation which remains is an initial state interaction of the beam particle inside the nucleus, before the formation of the J/ψ. Such an interaction is excluded if the J/ψ production mechanism is only parton fusion [24].

We conclude that a new mechanism appears at large x_F and low P_T, in which the incident hadron is absorbed before the creation of the J/ψ. Due to the similarity of this behaviour with the diffractive inclusive production (large x_F, low P_T and screening), we have called this mechanism the "diffractive component" of the production mechanism. The parton fusion production is called in the following the "hard component", in reference to the hardness of the interaction.

5.4 Quantitative estimations of the diffractive component

The two components of the production mechanism are characterized by two different nuclear dependances. We call α and β respectively the exponents of the nuclear effects for the hard and the diffractive component. We have the following relations :

$$\sigma(\pi H_2) = \sigma_h + \sigma_d$$
$$\sigma(\pi Pt) = A^{\alpha}(0.4\,\sigma_h + 0.6\,\sigma'_h) + A^{\beta}\sigma_d \qquad (5.4)$$

where σ_h and σ_d are respectively the hard and diffractive component on a proton target, and σ'_h is the hard component on a neutron target.

In the system of equations (5.4), each of the five quantities α, β, σ_h, σ'_h and σ_d are unknown, for only two equations.
However, we shall use the following procedure in order to extract the x_F distributions of the two components :

1) α is extracted from the behaviour of R at $x_F = 0$.
2) β is calculated using a standard rescattering model.
3) σ_h and σ_d are extracted by solving the system of equations (5.4) using the ratio σ'_h/σ_h expected from the parton fusion model described in section 7 (this is a small correction, less than 10%).

1) We use the fact that $d\sigma_d/dx\ (x_F = 0) = 0$, since σ_s is supposed to be a purely diffractive component. All the data sets agree for the value of α and we deduce an average value :

$$\alpha = 0.972 \pm 0.008$$

We have used the Glauber-Matthiae [25] density of the nuclear matter to calculate the correspondance between α and the absorption cross section of the ψ. This value of α corresponds to :

$$\sigma_{abs}(\psi + \text{nucleon}) = 2.2 \pm 0.7 \text{ mb}$$

which is in excellent agreement with the photoproduction measurements.

2) To evaluate β we use the diffusion model of Kölbig and Margolis [26] with the known values of the π-nucleon and p-nucleon cross sections at our energies (respectively 24 and 39 mb). This gives :

$\beta = 0.77 \pm 0.01$ for incident pions

$\beta = 0.71 \pm 0.01$ for incident protons

3) We can now extract σ_h and σ_d from Eq.(5.4), using the experimental x_F distributions. The results are shown on Fig. 5 for σ_d where we can also see the fraction of diffractively produced J/ψ; we obtain after integration on $x_F > 0$ the following fraction of J/ψ's produced by the diffractive component :

$$\frac{\sigma_d}{\sigma_h + \sigma_d} = \begin{array}{ll} 0.18 \pm 0.03 & \text{for incident pions at all energies} \\ 0.29 \pm 0.06 & \text{for incident protons at 200 GeV/c} \end{array}$$

6) TOTAL CROSS SECTION FROM VARIOUS INCIDENT PARTICLES

We give in Table 4 the J/ψ production cross sections, integrated over $x_F > 0$, for incident $\pi^{\pm}$ mesons on hydrogen and Platinum. What is given is in fact $B\sigma$ where $B(\psi \to \mu^+\mu^-) = 7.4 \pm 1.2\%$, since we detect only the dimuon decay channel of the J/ψ.

We give in Table 5 the values of the cross section ratios of J/ψ from various incident particles, with respect to the π^- induced cross section at the same energy. It is worth noting that the π^+/π^- cross section ratio on Platinum has a very small error. We have in fact used both our targets in order to extract this π^+/π^- ratio with such a precision (see ref. [23] for details). This has been used to connect the luminosities between positive and negative beams by using the J/ψ as "monitor".

In Table 6 we give the evaluation of $\sigma_{h,\bar{p}}/\sigma_{h,p}$ where σ_h is the "hard" component defined in section 4 : this ratio will be used in the following section to separate the gluon-gluon from quark-antiquark fusion in the hard component of the cross section.

7) x_F DISTRIBUTIONS OF THE HARD COMPONENT AND GLUON STRUCTURE FUNCTIONS

From the results of section 4, we can also extract the x_F distribution of the "hard" component of the hadronic J/ψ production.

These cross-sections are given in Fig. 7 for incident $\pi^{\pm}$ and protons at 200 GeV/c. If this "hard" cross-section is interpreted as coming from constituent fusion, we can derive the gluon structure functions in the proton and in the pion, since valence and sea quark distributions are known from other experiments.

7.1 Direct and indirect production

In fact this "hard" production may come either from direct fusion of constituents giving a J/ψ, or from the decay cascade of various charmonium states - in practice ψ' and χ states. The CERN WA11 experiment has given [10] precise evaluations of these cascade mechanism. They find that 17.7 ± 3.5% of J/ψ come from the χ_1 (3510) state, 12.8 ± 2.3% from the χ_2 (3555) and 8% from the ψ'. The χ_0 (3415) state does not decay sufficiently in to the J/ψ to contribute ($B(\chi_0 \to \psi\gamma) = 8 \pm 2\ 10^{-3}$).

In evaluating the x_F distribution of the J/ψ's produced indirectly, we have taken into account the kinematics of the electromagnetic decay $\chi \to \psi\gamma$, using the formula of ref.[27].

7.2 General notations

We write the "hard" cross section for the direct production of a state A as follows :

$$\frac{d\sigma}{dx_F} = \sigma_0 \left[\xi\, F_{q\bar{q}}(x_F) + F_{gg}(x_F)\right] \qquad (7.1)$$

where $\sigma_0 = \dfrac{4\pi^2\, G_{gg}}{M^2}$ is the elementary cross section of the the process gluon + gluon → A, M is the mass of A

$\xi = \dfrac{G_{q\bar{q}}}{G_{gg}}$ is the ratio of the effective coupling constants of $q\bar{q}$ and gg

$$F_{q\bar{q}}(x_F) = \sum_{q=u,d,s} \frac{B_q(x_1)\, T_{\bar{q}}(x_2) + B_{\bar{q}}(x_1)\, T_q(x_2)}{x_1 + x_2}$$

$$F_{gg}(x_F) = \frac{B_g(x_1)\, T_g(x_2)}{x_1 + x_2} \qquad (7.2)$$

with $x_1 = \frac{1}{2}\,(x_F + \sqrt{x_F^2 + 4M^2/s})$

and $x_2 = \frac{1}{2}\,(-x_F + \sqrt{x_F^2 + 4M^2/s})$

where B_q, B_g are the structure functions of quarks (resp. gluons) with fraction of momentum x_1 in the beam particle, and T_q, T_g in the target particle with momentum fraction x_2.

These expressions have to be explicited using the detailed parametrizations of the structure functions.

The same equation (7.1) holds for direct ψ' production, using the mass of the ψ' in equation (7.2). For χ_1 production, only $Fq\bar{q}$ contributes, since the χ_1 couples directly to $q\bar{q}$ and for χ_2, only F_{gg} contributes. We fix the relative values of the s_0's in order to reproduce the observed indirect yields of J/ψ's (see section 7.1).

7.3 Structure functions at $Q^2 = M_\psi^2$

7.3.1 Valence structure functions in the nucleon

We have extracted from neutrino deep-inelastic scattering data (Collaboration WA1 at CERN, ref.[28]), a standard parametrization of the valence structure functions. These functions are normalized to the number of quarks, and calculated at $Q^2 = 9.59$ GeV^2/c^4(since we are at the J/ψ mass) according to the measured scaling violations. The resulting parametrization is

$$u(x) = 2.48\, x^{0.56}\,(1 - x)^{2.61}$$

$$d(x) = 1.43\, x^{0.56}\,(1 - x)^{3.61}$$

7.3.2 Sea structure functions in the nucleon

We use the experimental result for the strange component of the sea :

$$\bar{s}(x) = 0.25\,[\bar{u}(x) + \bar{d}(x)]$$

to introduce a unique paramerization for the sea contribution, supposing $\bar{u}(x) = \bar{d}(x)$. We use the experimental value given in ref.[28] at Q^2 =

9 GeV² for the whole sea :

$$S(x) \equiv \bar{u}(x) = \bar{d}(x) = 2\bar{s}(x) = 0.2\ (1 - x)^{8.7}$$

These parametrizations of the valence and sea quarks give 37.5% of the proton momentum carried by valence quarks, 10.2% by the sea and 52.3% by the gluons.

7.3.3 Structure functions of the quark in the pion

We use the structure functions measured in this NA3 experiment at the same energies, from Drell-Yan events [29]. These functions have been measured at $M^2 = 25$ GeV², but the scaling violations have not yet been measured. To obtain the pion structure functions at $Q^2 = M_\psi^2$ we use the predictions of Buras-Gaemers [30] and obtain:

$$v_\pi(x) = 0.52\ x^{0.4}\ (1-x)^{0.78}$$
$$s_\pi(x) = 0.238\ (1-x)^{8.7}$$

The sea structure function is poorly known, but however, it does not contribute significantly to the J/ψ production at $x_F > 0$.

This parametrization corresponds to 36% of the pion momentum carried by valence quarks, 15% by sea quarks and 49% by gluons.

7.3.4 Parametrization of the gluon structure functions

In Eq.(7.1) we have only to introduce the unknown gluon structure functions. We choose a Buras-Gaemers parametrization for gluons

in the proton: $G_p(x) = A_p\ (1-x)^{g_p}$

in the pion : $G_\pi(x) = A_\pi\ (1-x)^{g_\pi}$

7.4 Results

We have performed a simultaneous fit of $d\sigma/dx_F$ from incident protons at 200 GeV/c, and of $\sigma(\bar{p})/\sigma(p)$ (which depends strongly on the parameter ξ of Eq. 6.1) to extract the following values:

$$\xi = 1.20 \pm 0.5$$
$$\sigma_o = 7.0 \pm 0.3\ (\text{stat.}) \pm 1.4\ (\text{syst})\ \text{nanobarns}$$
$$g_p = 5.16 \pm 0.21$$

This value of g_p is fairly compatible with the value obtained in neutrino deep inelastic data [31] which gives $g_p = 5.5$ at $Q^2 = 9.6$ GeV^2 (from a fit of the complicated formula of ref.[31]).

For incoming pions, we fix $g_p = 5.16$ and fit simultaneously all our pion data (150 GeV/c π^-, 200 GeV/c π^+ and π^-, 280 GeV/c π^-). We obtain:

$$g_\pi = 2.38 \pm 0.05 \text{ (statistical error only).}$$

We have also left σ_0 free for each data set. The obtained values are compatible together (see table 7) inside the uncertainties on the luminosities, which are rather large. But the value for π^+ and π^- at 200 GeV are compatible within the 1% relative error quoted in table 5.

To estimate systematical errors on g_p and g_π we have tried several changes in some important parameters:

- A major change in the χ_1 and χ_2 contribution to the J/ψ production (10% instead of 18%) gives $g_p = 5.23 \pm 0.22$ and g_π 2.45 ± 0.06.
- If we suppose that the χ_1 and χ_2 are both produced from gluon fusion and quark fusion, with the same ratio ξ than the J/ψ, we find $g_p = 5.04 \pm 0.2$ and $g_\pi = 2.34 \pm 0.05$.
- If we change considerably the valence quark structure functions, taking for instance $u(x) \propto \sqrt{x}(1-x)^3$ in the proton and $v_\pi(x) \propto \sqrt{x}(1-x)$ in the pion, we find $g_p = 5.08 \pm 0.22$ and $g_\pi = 2.83 \pm 0.08$.

To conclude, we estimate that systematical errors may be estimated around ± 0.1 on g_p and g_π and we give finally

$$g_p = 5.1 \pm 0.2 \text{ (stat)} \pm 0.1 \text{ (syst.)}$$
$$g_\pi = 2.38 \pm 0.06 \text{ (stat)} \pm 0.1 \text{ (syst.).}$$

The quality of the fits can be seen in table 7 where we have quoted the χ^2 for each individual data set, and on figures 7a and 7b, where the data for the hard component and the curves resulting from the fit are given.

7.5 Comparison with previous results

As noted in section 7.4, the value of g_p is fairly compatible with Deep Inelastic Scattering data. Concerning g_π, the CERN WA11 experiment [32] has obtained the value $g_\pi = 1.9 \pm 0.2$, supposing that all J/ψ's are produced by gluon fusion. Our data have shown that this is not the case, and furthermore the WA11 used only a Be target and was thus unable to give evidence for a diffractive contribution to the cross section.

8) X_F DISTRIBUTIONS FROM KAONS AND ANTIPROTONS

8.1 Incident kaons

We give on Fig. 8 the ratios $\sigma(K^{\pm}Pt \to \psi)/\sigma(\pi^{\pm}Pt \to \psi)$ as a function of x_F. These ratios are independant of acceptance corrections, since they come from data which have been taken simultaneously in the same apparatus; they depend only for the overall normalization on the incident particle fluxes.

Since the fusion of strange quarks does not contribute much to the cross section, the observed effect has mainly two sources :

a) The difference of the $\bar{u}$-quark structure function, as it was measured in the Drell-Yan continuum [33] :

$$\frac{\bar{u}_K(x_F)}{\bar{u}_\pi(x_F)} \propto (1 - x)^{0.18}$$

b) The amount of gluons inside the kaon, as well as their structure function, can be different from the pion.

We have used the same shape for the gluon structure functions in the pion and in the kaon, varying the normalisation in order to obtain the curves on Fig. 8. The fraction of momentum carried by gluons is respectively 53%, 48.5%, 44% and 40% when going from the lower to the upper curve. Let us recall that the structure functions used for the pion left 50% of the momentum carried by the gluons.

In conclusion, our data confirm the difference of structure inside the kaon and the pion, but no strong constraints can be put on the fraction of momentum carried by the gluons in the kaon, although the curve corresponding to a fraction of 48.5% gives the best agreement with our data.

8.2 Incident antiprotons and protons :

From the results of Sect. 6 we can obtain an absolute prediction for the ratio $\sigma_{\bar{p}}/\sigma_{p}$ as a function of x_F.

We give in Fig. 9 the experimental data at 150 GeV/c together with the curve deduced from the parton fusion model, using our gluon structure function.

In Fig. 10 we also give the $\bar{p}/\pi^-$ and p/π^+ ratios as a function of x_F, showing how much steeper the distribution for incident baryons is than for mesons. This result is identical to that of ref. [14] at 125 GeV/c.

9) TRANSVERSE MOMENTUM DISTRIBUTIONS

In Figs. 11a and 11b we give the differential cross section $d\sigma/dp_T$ for the J/ψ's produced respectively on hydrogen and platinum. The mean values of P_T and P_T^2 integrated for $x_F > 0$ are given in table 7.
One can note that these values are rather high as compared to low mass hadrons inclusive production, but are in the same range as those obtained for the continuum in this mass region [13,34].

As for the continuum dimuons, the P_T of the J/ψ's is lower for incident protons than for incident pions.

The behaviour of $< P_T >$ and $< P^2_T >$ as a function of x_F is given in figure 12, showing a significant decrease at large x_F, as here diffractive production begins to dominate.

It is stated in ref. [35] that high P_T production of J/ψ's could occur through gg and gq interactions, which should give the same cross section for protons and antiproton induced reaction. One can see on Fig. 13 that no obvious trend is observed for a variation of the ratio $\sigma_{\bar{p}}/\sigma_p$ as a function of P_T.

10) ANGULAR DISTRIBUTIONS

As for many experiments, the NA3 spectrometer has a rather limited acceptance for very asymetric decays at the mass of the J/ψ. This means that the determination of the shape of the angular cos θ distribution is rather difficult.

Our only data set for which the acceptance enables this is that for 280 GeV pions, because of the larger boost.

We have used for a definition of θ and ϕ the Collins-Soper frame [36] and we use the following parametrization of the angular distribution :

$$\frac{1}{\sigma}\frac{d^2\sigma}{d\cos\theta\, d\phi} = \frac{3}{2(3+\lambda)}\left(1 + \lambda\cos^2\theta + \beta\sin 2\theta\cos\phi + \gamma\sin^2\theta\cos 2\phi\right)$$

The result for the whole region $x_F > 0$, integrated over P_T is :

On hydrogen	On platinum
λ = -0.20 ± 0.06	λ = -0.31 ± 0.02
β = 0.00 ± 0.02	β = 0.02 ± 0.01
γ = 0.009 ± 0.014	γ = -0.007 ± 0.004
χ^2 = 679/653 D.F.	χ^2 = 1516/835 D.F.

The errors quoted here are statistical only. The systematics on these parameters are very difficult to estimate. They are very small on β and γ, as the ϕ - acceptance is flat, but can be of the order of 0.1 on λ, due to the decrease of the acceptance at large $|\cos\theta|$. Figure 14 shows $dN/d\cos\theta$ on platinum together with the result of the fit and the acceptance.

An attempt has been made to evaluate the parameters λ, β and γ as a function of x_F and P_T. The result is given on figure 15a and 15b*). It shows a clear trend for λ to depart from 0 at large x_F as well as at x_F near 0. This result is comparable to that of ref. [37]. The parameters β and γ are both compatible with 0 for all kinematical regions, contrary to what happens for the continuum dimuons [38].

Precise theoretical calculations of these parameters have been made for several fusion subprocesses involving an intermediate χ state [39], which show that λ is very much process-dependent, and stress the fact that it is very difficult to get a clear prediction for all J/ψ's together. A more refined experiment should be made, measuring the cascade photons with a good precision in order to separate χ_1 and χ_2 states and to obtain the 3 particle angular correlation between the muons and the photon [40]

11) CONCLUSIONS

From our analysis of a high statistics of J/ψ's produced by various hadron beams at high energy, we have pointed out that about 18% of the J/ψ's at $x_F > 0$ are produced by a diffractive process. It is now still difficult to explain how this production takes place, but theoretical models are on the way [21, 24].

The hard component of J/ψ production has been analysed in the framework of a parton fusion model, leading to the evaluation of the gluon structure function.

---

*) No constraints were put on the fitted parameters, which explains why λ is out of the physical region ($|\lambda| < 1$) for large x_F.

Less information can be given by transverse momentum and angular distribution, but nevertheless the theoretical predictions should explain as well the high mean P_T of the J/ψ as the variation of the λ parameter as a function of x_F. The fact that $\lambda \to -1$ where diffractive production dominates can be a guide for the explanation requested above.

We would like to thank the SPS staff for operating the accelerator and the beam line during the two years of this experiment. The whole technical staff of NA3 has largely contributed to this experiment. We acknowledge in particular R. Lorenzi, R. Hammarström and the "Saclay antenne" at CERN directed by G. Bertalmio for their constant help before and during the runs and M. Décamp for her efficient work in all adminstrative business and typing of the paper.

REFERENCES

[1] J.J Aubert et al., Phys. Rev. Lett. 33 (1974) 1404.
J.E. Augustin et al., Phys. Rev. Lett. 33 (1974) 1406.

[2] J. Badier et al., Nucl. Instr. and Meth., 175 (1980) 319.

[3] Y.U. Antipov et al., Phys. Lett. 72B (1977) 278
Phys. Lett. 76B (1978) 235.

[4] Y.U. Antipov et al., Phys. Lett. 60B (1976) 309;
Y.B. Bushnin et al., Phys. Lett. 72B (1977) 269.

[5] M.J. Corden et al., Phys. Lett. 68B (1977) 96.

[6] M.J. Corden et al., Phys. Lett. 96B (1980) 411
Phys. Lett. 98B (1980) 220

[7] Ph. Charpentier, Proceedings of the first Moriond Workshop on Lepton Pair production, Les Arcs 1981, J. Tran Thanh Van Editor.

[8] M.J. Corden et al., Phys. Lett. 110B (1982).

[9] M.A. Abolins et al., Phys. Lett. 82B (1979) 145.

[10] Y. Lemoigne et al., Phys. Lett. 113B (1982) 509.

[11] J.G. Mac Ewen et al., Phys. Lett. 121B (1983) 198.

[12] K.J. Anderson et al., Phys. Lett. 36 (1976) 237;
J.G. Branson et al., Phys. Lett. 38 (1977) 1331.

[13] J.G. Branson et al., Phys. Lett. 38 (1977) 1334.

[14] E. Anassontis et al., FERMILAB - Conf - 82/49 - EXP.

[15] J.J. Aubert et al., CERN preprint EP/82-152, to be published in Phys. Lett. B.

[16] R.L. Anderson, SLAC-Pub (1976) 1741.

[17] V. Barger and R.J.N. Phillips, Nucl. Phys. B97 (1975) 452.

[18] R.J.N. Phillips, Rapporteur's talk at the XX INternational Conf. on High Energy Physics, Madison, Wisconsin, July 1980

[19] M. Glück and E. Reya, Phys. Lett. 79B (1978) 453.

[20] M.J. Teper, Phys. Lett. 78B (1978) 148

[21] S.J. Brodsky et al., Phys. Rev. D23 (1981) 2745.
This reference points out that a large suppression factor takes place to avoid large diffractive J/ψ production, but in particular the mass suppression does not seem to be as large [23] and could allow for some non negligible "intrinsic" J/ψ.

[22] J. Badier et al., Phys. Lett. 104B (1981) 335.

[23] Ph. Charpentier, Université Paris-Sud, thèse avril 1983 (unpublished).

[24] C. Michael, Proceedings of the Moriond Workshop on Gluons, La Plagne 1983, J. Tran Thanh Van editor.

[25] R.J. Glauber et G. Matthiae, Nucl. Phys. B21 (1970) 135.

[26] K.S. Kölbig and B. Margolis, Nucl. Phys. B6 (1968) 85.

[27] G.E. Carlson and R. Suaya, Phys. Rev. D18 (1978) 760.

[28] F. Eisele, Rapporteur's talk at the International Conference on High Energy Physics, Paris, July 26-31 1982; proceedings page-337.

[29] J. Badier et al., Preprint CERN EP/83-48, March 1983, to be published in Zeitschrift für Physik C

[30] A.J. Buras and K.J.F. Gaemers, Nucl. Phys. B132 (1978) 249.

[31] H. Abramowicz et al., Zeit. für Physik C12, 289 (1982).

[32] J.G. Mc Ewen et al., Phys. Lett. 121B (1983) 198.
V. Barger et al., Zeitschrift für Physik C 6 (1980) 169.

[33] J. Badier et al., Phys. Lett. 93B (1980) 354.

[34] J. Badier et al., Phys. Lett. 117B (1982) 372.

[35] R. Baier and R. Rückel, Preprint BI-TP 81/06.

[36] J.C. Collins, D.E. Soper, Phys. Rev. D16 (1977) 2218.

[37] M.A. Abolins et al., Preprint DPhPE 78-05, August 1978.

[38] J. Badier et al., Zeitschrift für Physik C 11 (1981) 195.

[39] E.N. Argyres and C.S. Lam, Phys. Rev. D21 (1980) 143.

[40] E.N. Argyres and C.S. Lam, Preprint, State University of New-York, June 1982.

FIGURE CAPTIONS

Fig. 1 Dimuon mass spectrum from incident π^+ at 200 GeV/c.

Fig. 2 Ratio of J/ψ cross sections on hydrogen and platinum:
$R(x_F) = A \frac{d\sigma(H_2)}{dx_F} / \frac{d\sigma(Pt)}{dx_F}$ for the various π^+, π^-, p data of this experiment.

Fig. 3 Same as Fig. 2 for the ratio $R(P_T) = A \frac{d\sigma(H_2)}{dP_T} / \frac{d\sigma(Pt)}{dP_T}$

Fig. 4 Ratio $R(x_F)$ for different p_T slices

Fig. 5a,b) Diffractive component of the J/ψ production cross section $d\sigma_d/dx_F$ at 150 and 280 GeV from induced π^-;

c,d) Ratio $\frac{d\sigma_d}{dx_F} / \frac{d\sigma}{dx_F}$ at 150 and 280 GeV.

Fig. 6 Same as Fig. 5 for incident pions and protons at 200 GeV.

Fig. 7 Hard component $d\sigma_h/dx_F$ for incident protons (a) and pions (b) (the curves are the result of the fit described in the text. Dashed line: gluon-gluon fusion; dash-dotted line : $q\bar{q}$ fusion; full line : total).

Fig. 8 Ratio of K induced to π induced cross sections. The curves are the predictions described in the text for different normalisations of the gluons in the kaon.

Fig. 9 Ratio $\frac{d\sigma(\bar{p})}{dx^F} / \frac{d\sigma(p)}{dx^F}$ at 150 GeV/c. The curve is the absolute prediction using our fitted structure functions.

Fig. 10a) $\frac{d\sigma(\bar{p})}{dx_F} / \frac{d\sigma(\pi^-)}{dx_F}$ and b) $\frac{d\sigma(p)}{dx_F} / \frac{d\sigma(\pi^+)}{dx_F}$ at 150 and 200 GeV/c

Fig. 11 p_T distributions from various incoming particles
a) on H_2 target
b) on Pt target.

Fig. 12 $< P_T >$ and $< P_T^2 >$ as a function of x_F.

Fig. 13 Ratio $\sigma(\bar{p})/\sigma(p)$ at 150 GeV/c, as a function of p_T.

Fig. 14 Angular distribution $dN/d\cos\theta$ for incident 280 GeV π^- ($x_F > 0$).

Fig. 15 Variation of the λ, β and γ parameters of the angular distribution with
a) x_F
b) p_T
(only statistical errors on the fit are given).

TABLE 1.

Beam running conditions and luminosities on the platinum target.

Energy (GeV)	Max. intensity (particles/second)	Incident Particles (identified)	Luminosity on Pt target (cm^{-2})
200	$3.0\ 10^7$	π^- 96.3% K^- 3.1% $\bar{p}$ 0.6%	$9.6 \pm 1.0\ 10^{37}$ $1.3 \pm 0.2\ 10^{36}$ $5.9 \pm 0.9\ 10^{35}$
200	$5.5\ 10^7$	π^+ 36% p 60% K^+ 4%	$7.4 \pm 0.9\ 10^{37}$ $9.8 \pm 1.7\ 10^{37}$ $1.3 \pm 0.15\ 10^{37}$
150	$5.0\ 10^7$	π^- 93% K^- 5% $\bar{p}$ 2%	$5.1 \pm 0.7\ 10^{38}$ $1.6 \pm 0.24\ 10^{37}$ $6.0 \pm 1.0\ 10^{36}$
150	$5.0\ 10^7$	π^+ p K^+	$6.3 \pm 0.9\ 10^{36}$ $6.7 \pm 0.9\ 10^{36}$ $3.5 \pm 0.6\ 10^{35}$
280	$3.0\ 10^7$	π^- >99%	$2.78 \pm 0.25\ 10^{38}$

TABLE 2.

Number of J/ψ events obtained in this experiment

Momentum (GeV/c)	Target	π^+	K^+	p	π^-	K^-	$\bar{p}$
200	H_2	2407	359	2227	3157	-	-
200	Pt	104866	14690	80786	131062	1963	657
150	H_2	207	-	-	16952	487	208
150	Pt	7937	442	3453	601691	19190	6569
280	H_2	-	-	-	23350	-	-
280	Pt	-	-	-	511457	-	-

TABLE 3.

Values of the parameter α describing the nuclear dependance of J/ψ total cross sections: $\sigma(A) = A^{\alpha}\sigma_0$, obtained from our data.

Energy	Incident particle	α
150 GeV/c	π^-	0.95 ± 0.02
200 GeV/c	π^-	0.97 ± 0.02
	π^+	0.96 ± 0.02
	p	0.94 ± 0.03
280 GeV/c	π^-	0.96 ± 0.02

TABLE 4.

J/ψ production cross section
(Values of $B\sigma$, B = branching ratio of $\psi \to \mu^+\mu^-$, integrated over $x_F > 0$).

Incident particle	Momentum GeV/c	$\sigma(H_2)$ nb/proton	σ(Pt) nb/Pt nucleus
π^-	150	6.5 ± 0.9	884 ± 130
π^-	200	6.3 ± 0.8	960 ± 150
π^+	200	5.8 ± 0.8	976 ± 150
π^-	280	8.7 ± 0.8	1270 ± 120

TABLE 5.

Ratios of J/ψ production cross sections for various particles, with respect to π^- induced cross section at the same incident momentum.

Incident particle	Momentum GeV/c	H_2	P_T
K^-	150	0.89 ± 0.05	0.98 ± 0.05
$\bar{p}$	150	1.02 ± 0.1	0.90 ± 0.06
π^+	150	0.95 ± 0.03	1.010 ± 0.013
K^+	150	-	1.02 ± 0.10
p	150	-	0.42 ± 0.04
K^+	200	-	1.09 ± 0.12
$\bar{p}$	200	-	0.76 ± 0.09
π^+	200	0.92 ± 0.03	1.016 ± 0.006
K^+	200	0.81 ± 0.10	0.83 ± 0.10
p	200	0.58 ± 0.07	0.53 ± 0.05

TABLE 6.

Ratios of the hard component σ_h of antiprotons induced J/ψ, with respect to protons at the same incident momentum.

Incident momentum (GeV/c)	39.5 (Ref. 6)	150 (This exp.)	200 (This exp.)
$\sigma_h(\bar{p})/\sigma_h(p)$	5.6 ± 1.0	2.35 ± 0.3	1.46 ± 0.25

TABLE 7

Value of the parameter σ_0 of equation (7.1) obtained in the fit for each data set

Incident particle and energy	σ_0 (± stat. ± syst.)	χ^2/DF
p 200 GeV	7.0 ± 0.3 ± 1.4	15.4/10
π^- 150 GeV	9.6 ± 0.2 ± 1.3	44/20
π^- 200 GeV	8.3 ± 0.2 ± 0.9	9.5/10
π^+ 200 GeV	8.1 ± 0.2 ± 1.0	11.7/10
π^- 280 GeV	8.2 ± 0.2 ± 0.7	23/20

TABLE 8

Mean values of P_T and P_T^2 for $x_F > 0$

Particle	π^-	π^-	π^+	π^-	protons
Energy (GeV)	150	200	200	280	200
$< P_T >_{H_2}$	0.95 ± 0.02	1.01 ± 0.02	1.03 ± 0.02	1.06 ± 0.02	0.95 ± 0.02
$< P_T^2 >_{H_2}$	1.22 ± 0.05	1.40 ± 0.05	1.42 ± 0.05	1.52 ± 0.05	1.23 ± 0.05
$< P_T >_{Pt}$	1.06 ± 0.01	1.12 ± 0.01	1.13 ± 0.01	1.17 ± 0.01	1.08 ± 0.01
$< P_T^2 >_{Pt}$	1.49 ± 0.03	1.70 ± 0.03	1.71 ± 0.03	1.85 ± 0.03	1.57 ± 0.03

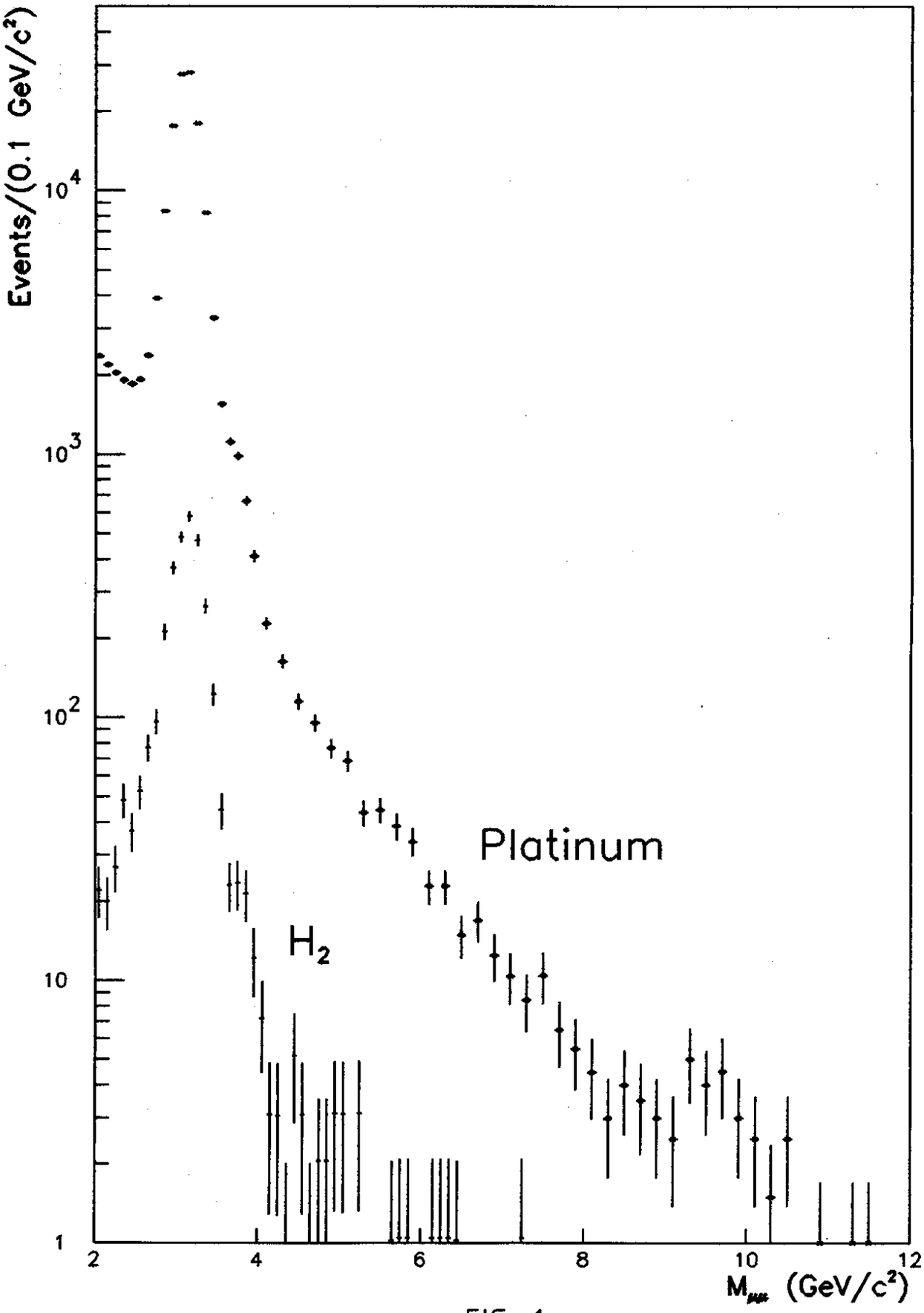
Events/(0.1 GeV/c²)
10⁴
10³
10²
10
1
2
4
6
8
10
12
M_μμ (GeV/c²)
Platinum
H₂

FIG. 1

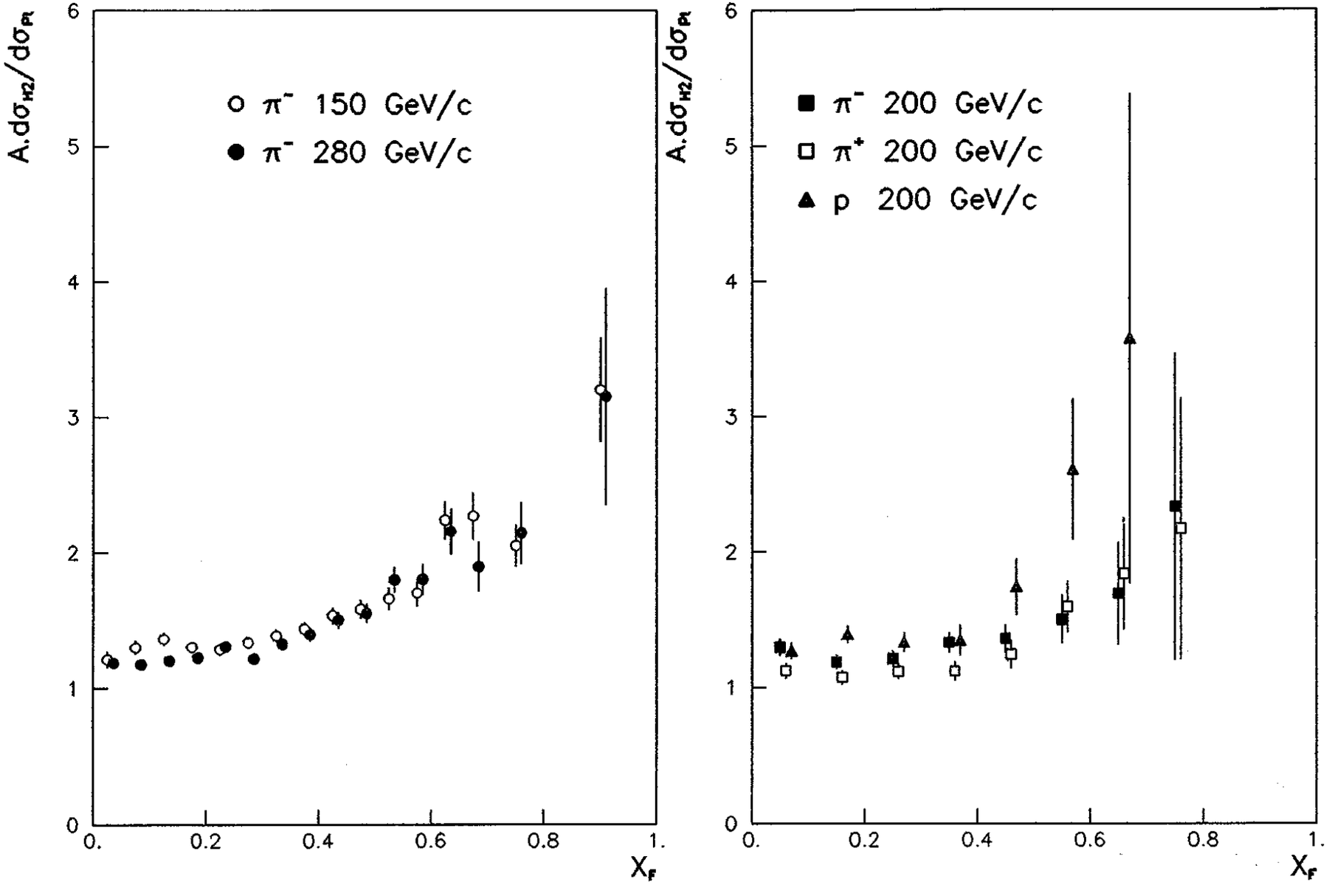
A.dσH2/dσPt
o π⁻ 150 GeV/c
● π⁻ 280 GeV/c
■ π⁻ 200 GeV/c
□ π⁺ 200 GeV/c
▲ p 200 GeV/c
0
1
2
3
4
5
6
0.
0.2
0.4
0.6
0.8
1.
XF

FIG. 2

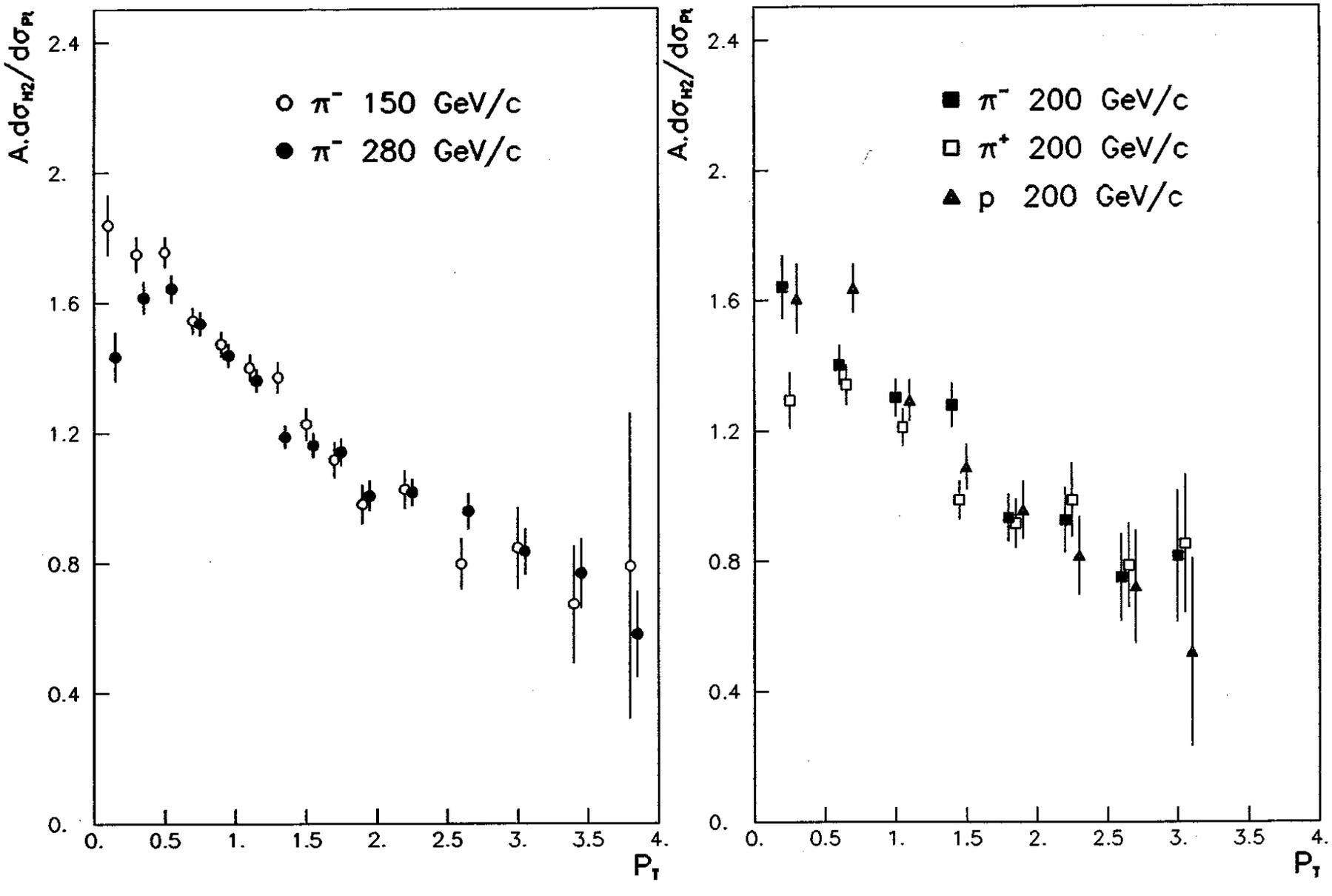
A.dσH2/dσPt
2.4
2.
1.6
1.2
0.8
0.4
0.
0.
0.5
1.
1.5
2.
2.5
3.
3.5
4.
PT
π⁻ 150 GeV/c
π⁻ 280 GeV/c
π⁻ 200 GeV/c
π⁺ 200 GeV/c
p 200 GeV/c

FIG. 3

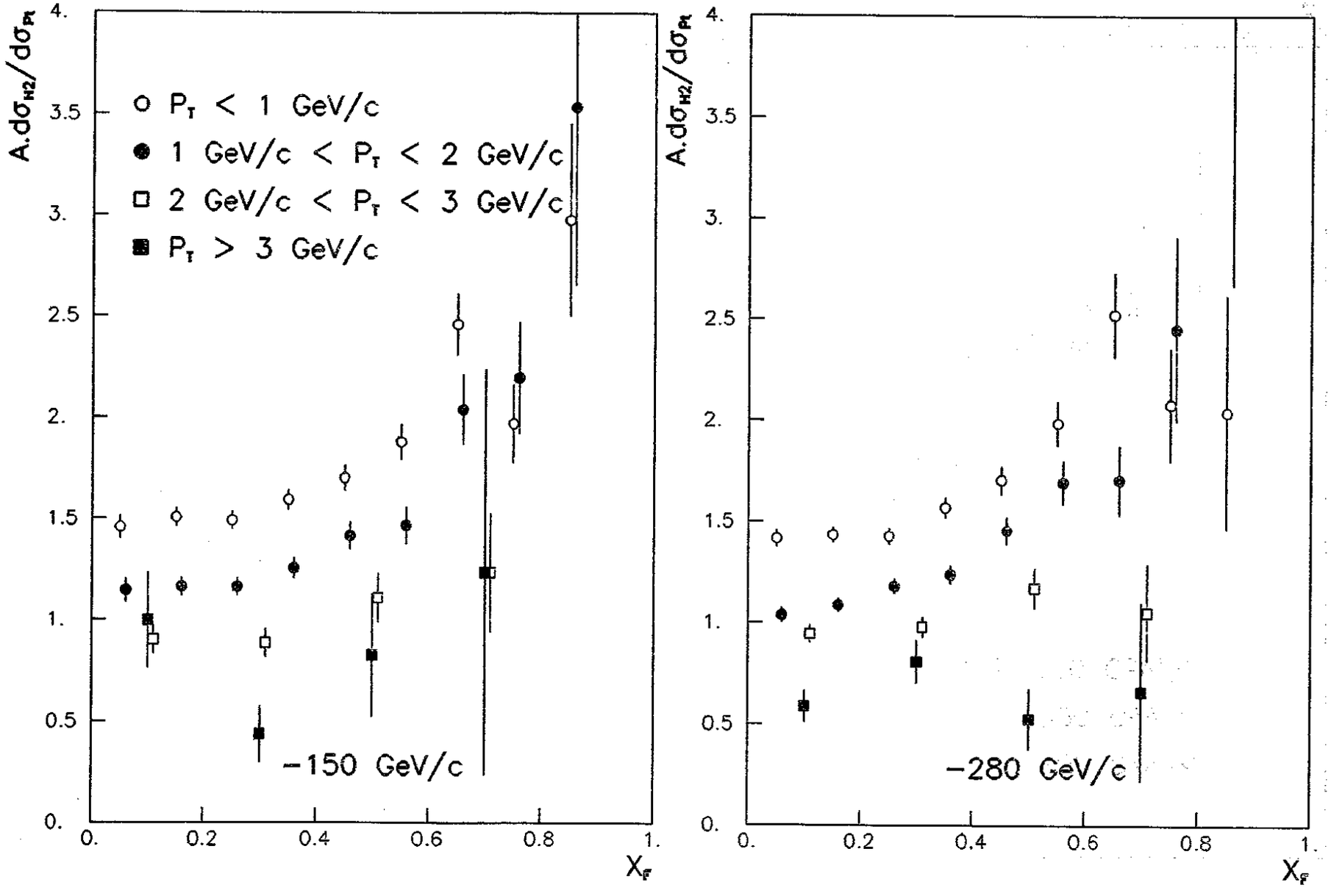
A.dσ_H2/dσ_Pt
4.
3.5
3.
2.5
2.
1.5
1.
0.5
0.
0.
0.2
0.4
0.6
0.8
1.
X_F
P_T < 1 GeV/c
1 GeV/c < P_T < 2 GeV/c
2 GeV/c < P_T < 3 GeV/c
P_T > 3 GeV/c
-150 GeV/c
-280 GeV/c

FIG. 4

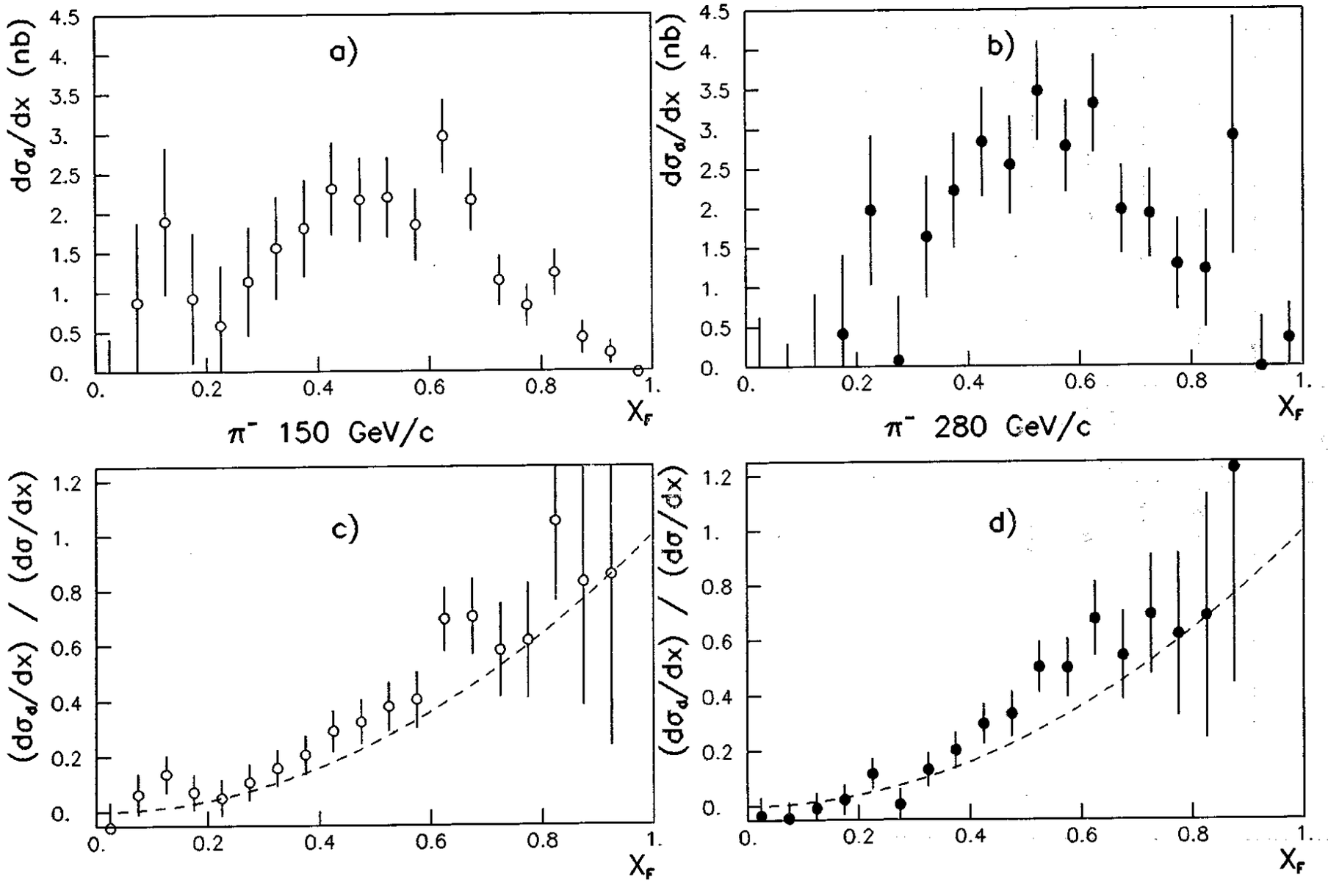
a)
b)
c)
d)
$d\sigma_d/dx$ (nb)
$(d\sigma_d/dx) / (d\sigma/dx)$
X_F
π^- 150 GeV/c
π^- 280 GeV/c

FIG. 5

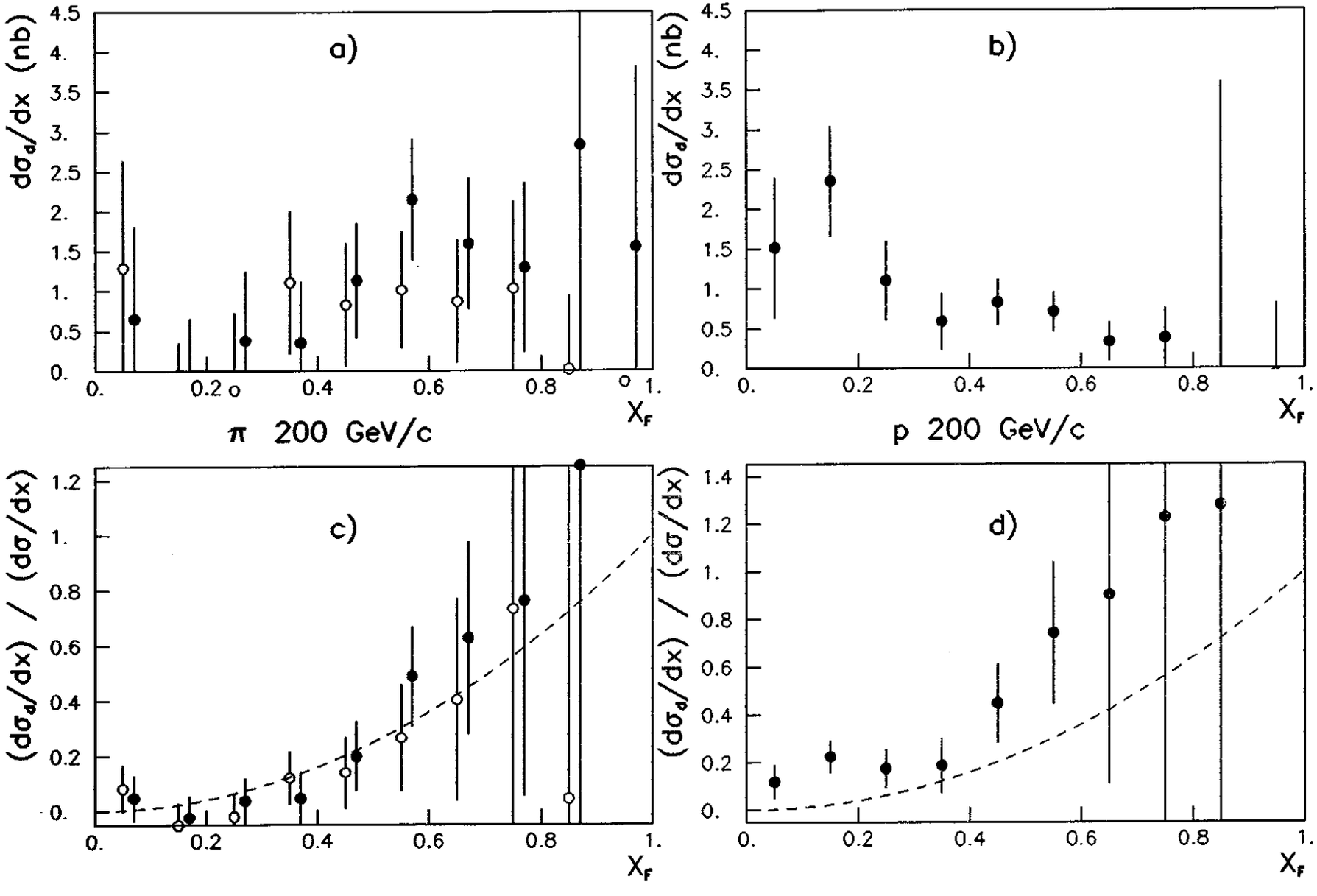
a)
b)
c)
d)
$d\sigma_d/dx$ (nb)
$(d\sigma_d/dx) / (d\sigma/dx)$
X_F
π 200 GeV/c
p 200 GeV/c

FIG. 6

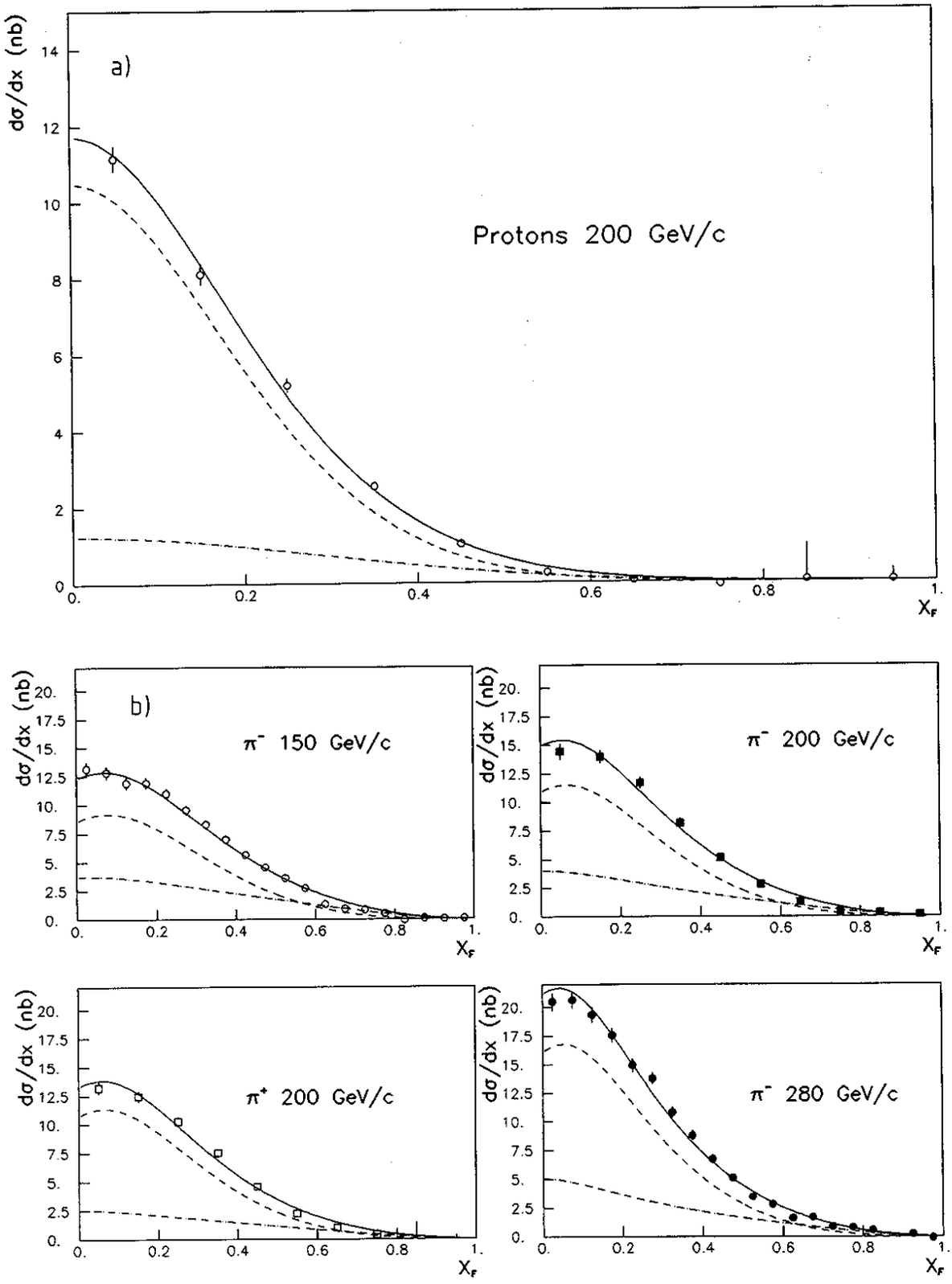
a)
Protons 200 GeV/c
dσ/dx (nb)
X_F
b)
π⁻ 150 GeV/c
π⁻ 200 GeV/c
π⁺ 200 GeV/c
π⁻ 280 GeV/c

FIG. 7

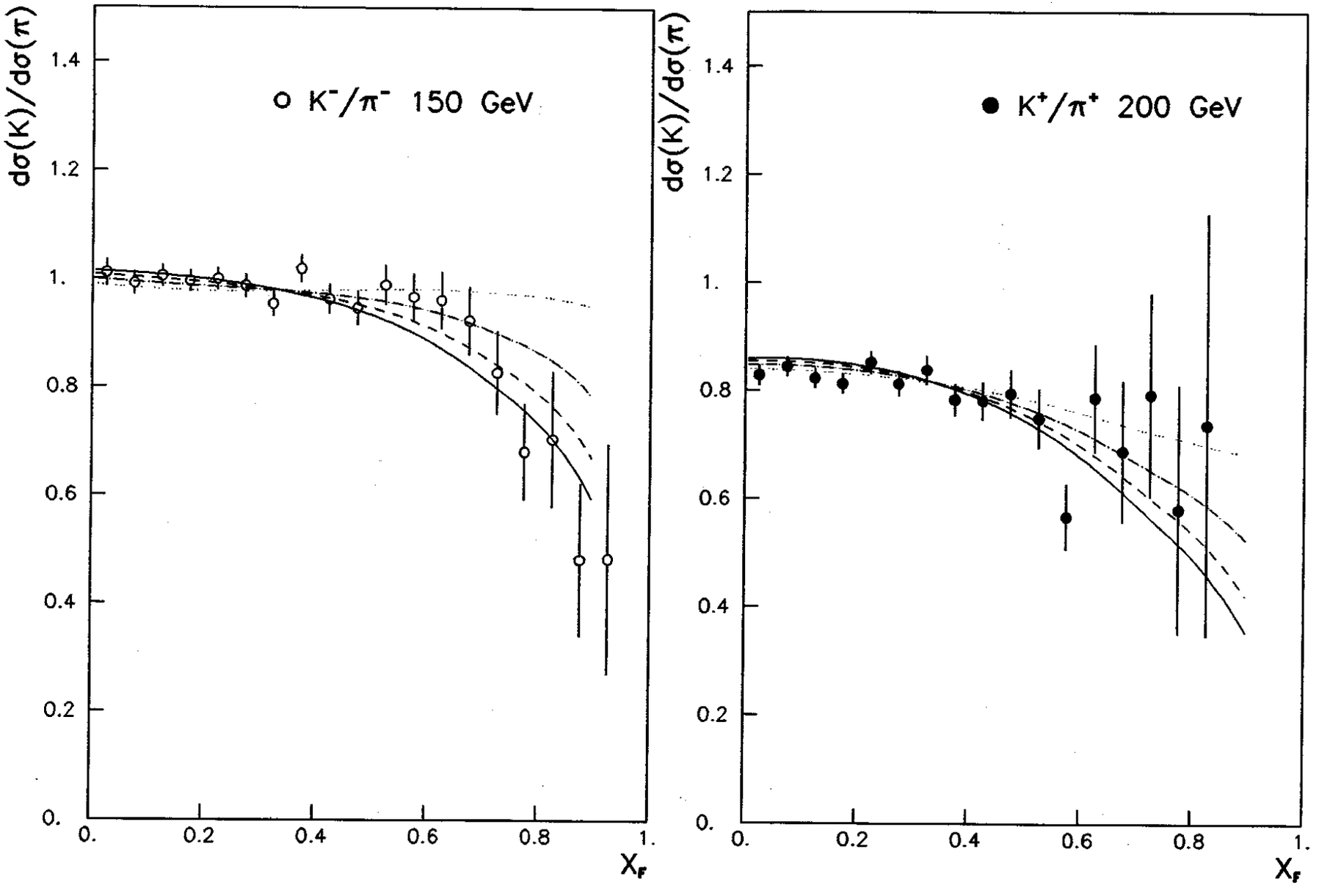

FIG. 8

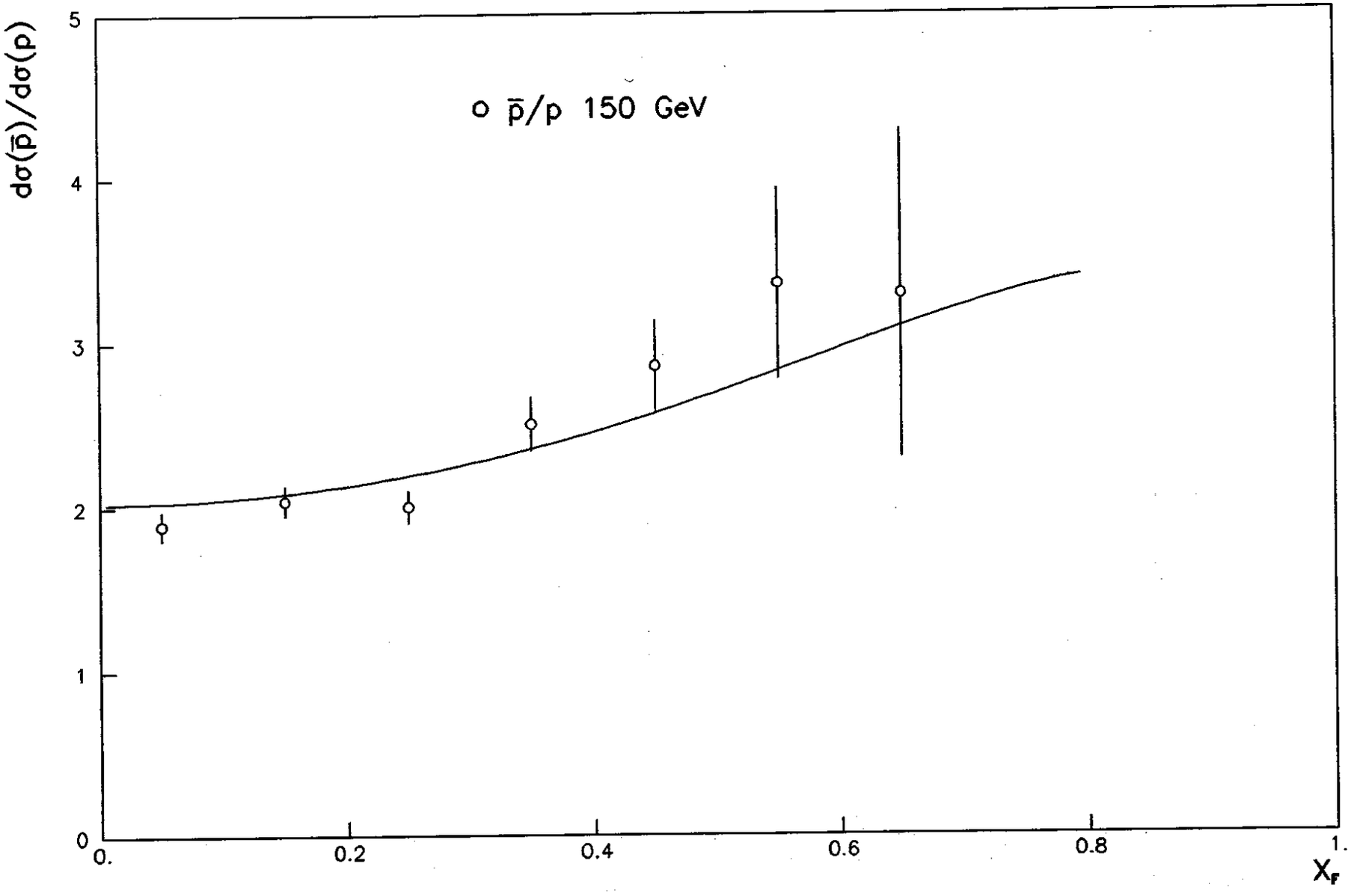

FIG. 9

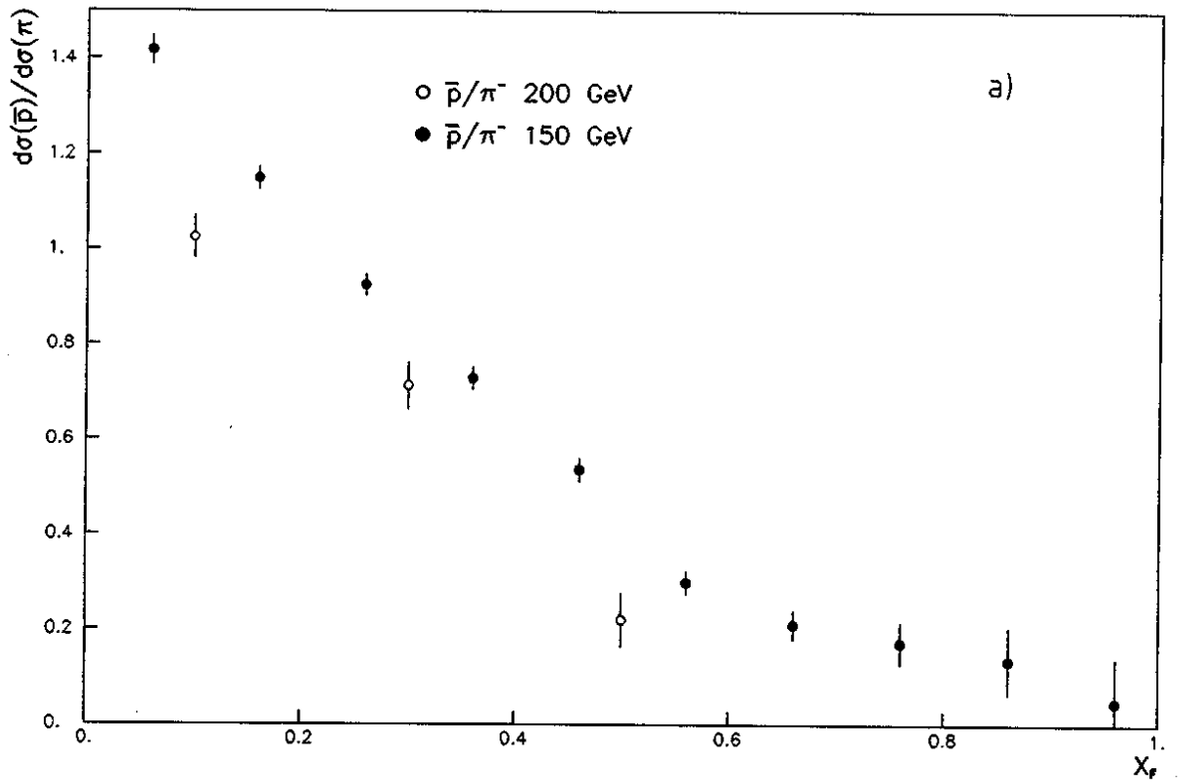
dσ(p̄)/dσ(π)
o p̄/π⁻ 200 GeV
● p̄/π⁻ 150 GeV
a)
0.
0.2
0.4
0.6
0.8
1.
1.2
1.4
X_F

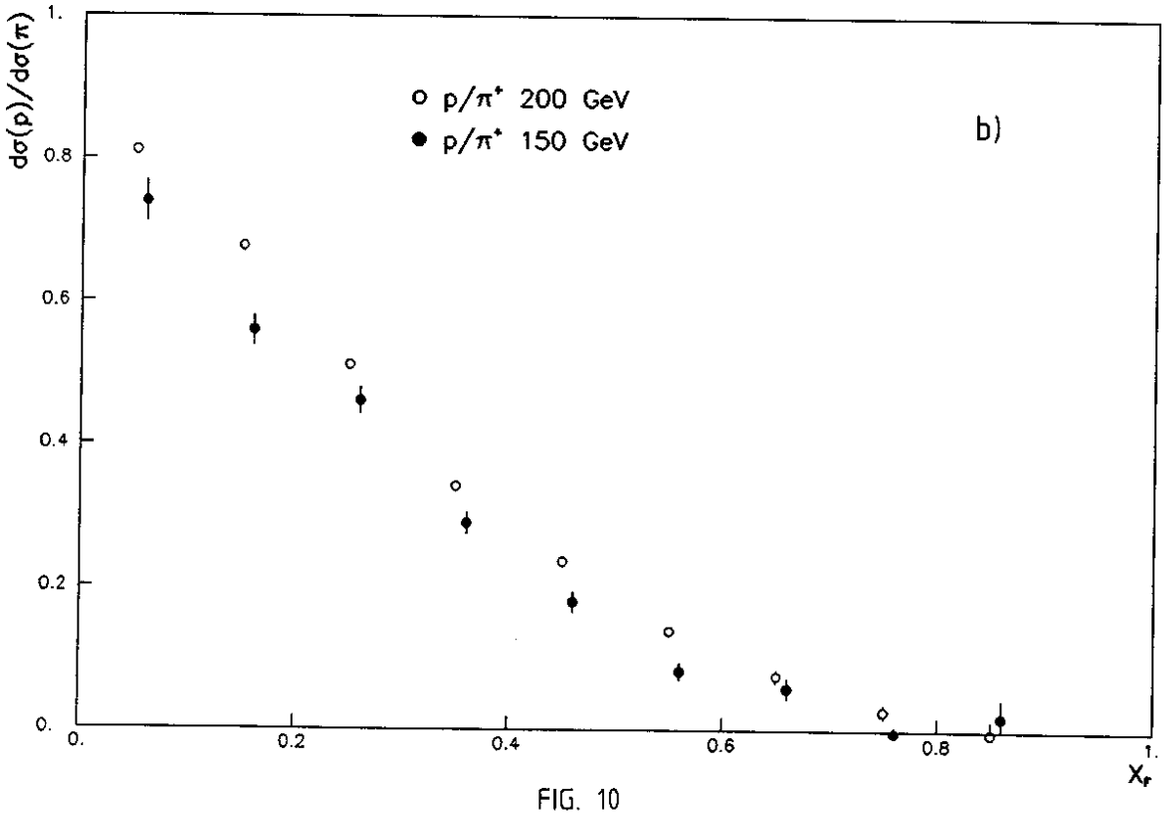
dσ(p)/dσ(π)
o p/π⁺ 200 GeV
● p/π⁺ 150 GeV
b)
0.
0.2
0.4
0.6
0.8
1.
X_F

FIG. 10

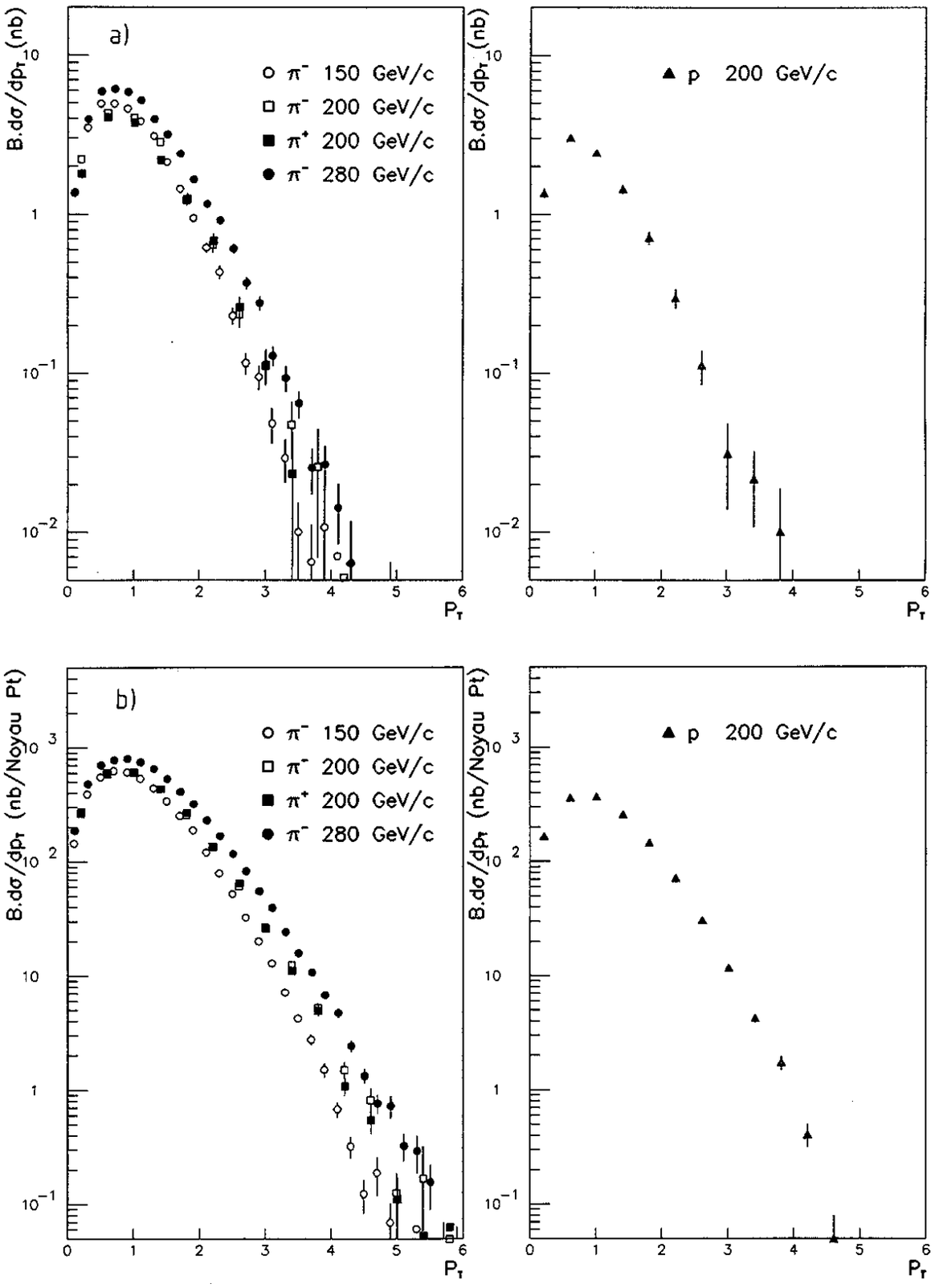
a)
B.dσ/dp_T (nb)
π⁻ 150 GeV/c
π⁻ 200 GeV/c
π⁺ 200 GeV/c
π⁻ 280 GeV/c
p 200 GeV/c
P_T
b)
B.dσ/dp_T (nb/Noyau Pt)

FIG. 11

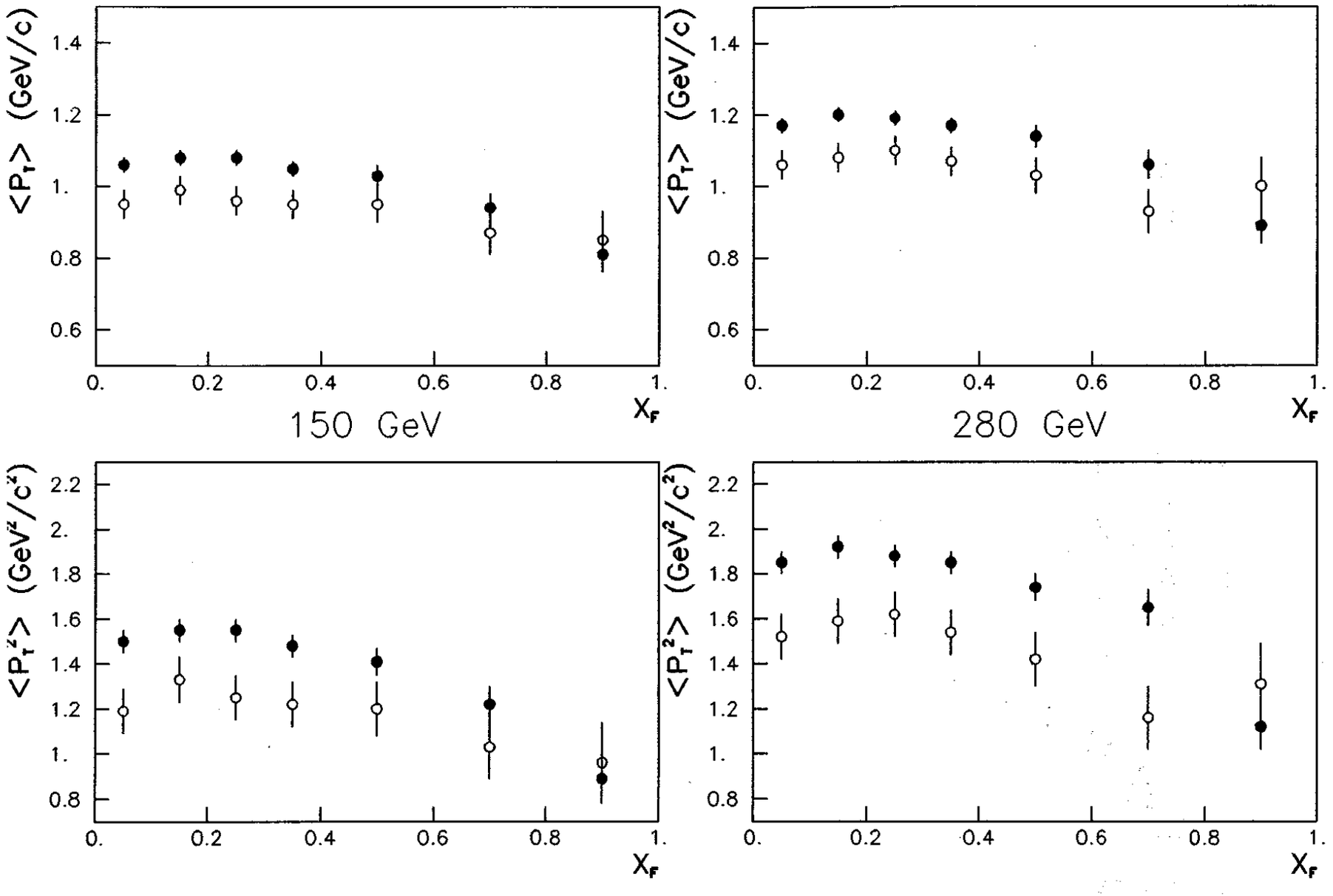
<P_T> (GeV/c)
1.4
1.2
1.
0.8
0.6
0.
0.2
0.4
0.6
0.8
1.
X_F
150 GeV
280 GeV
<P_T^2> (GeV^2/c^2)
2.2
2.
1.8
1.6
1.4
1.2
1.
0.8

FIG. 12

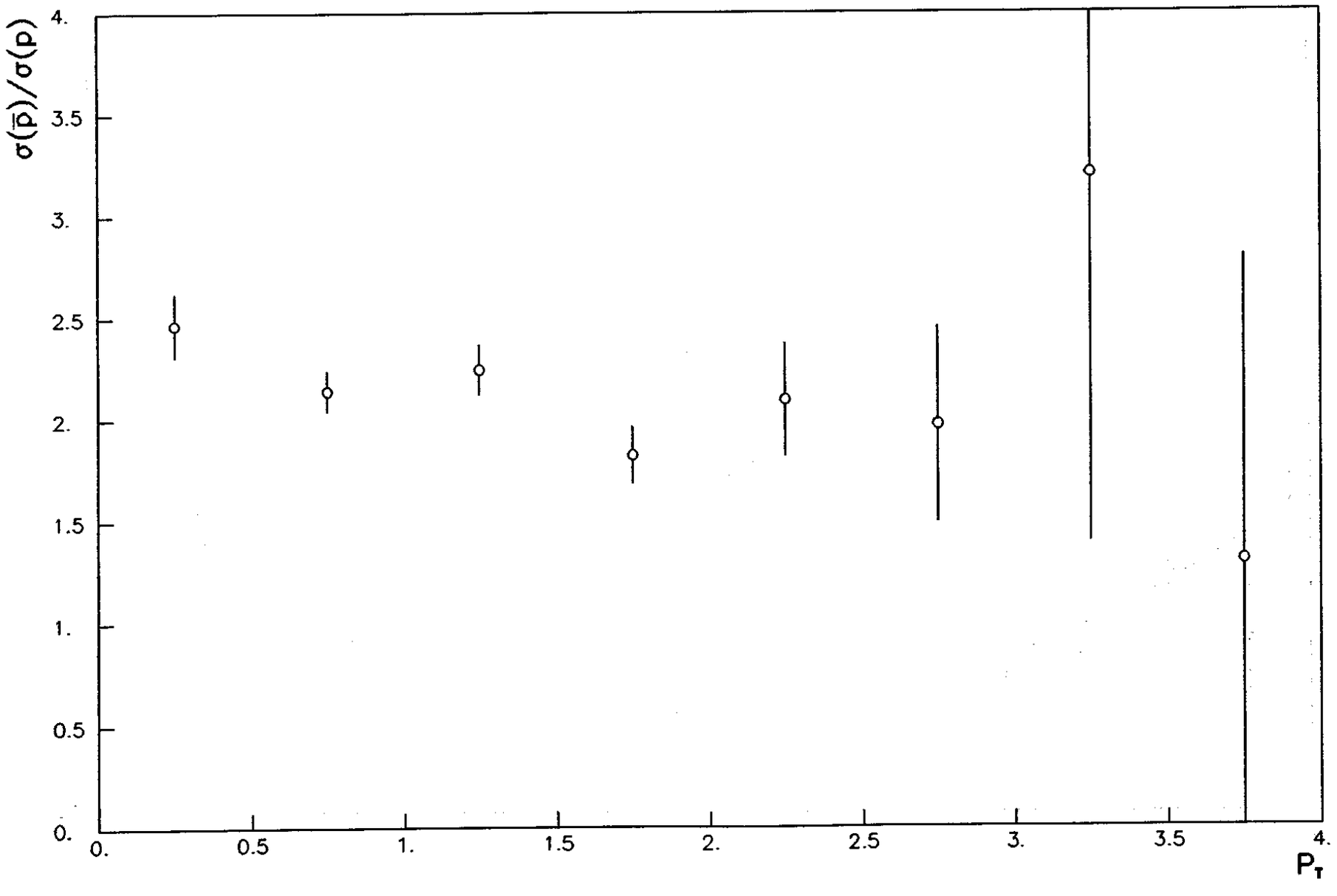

FIG. 13

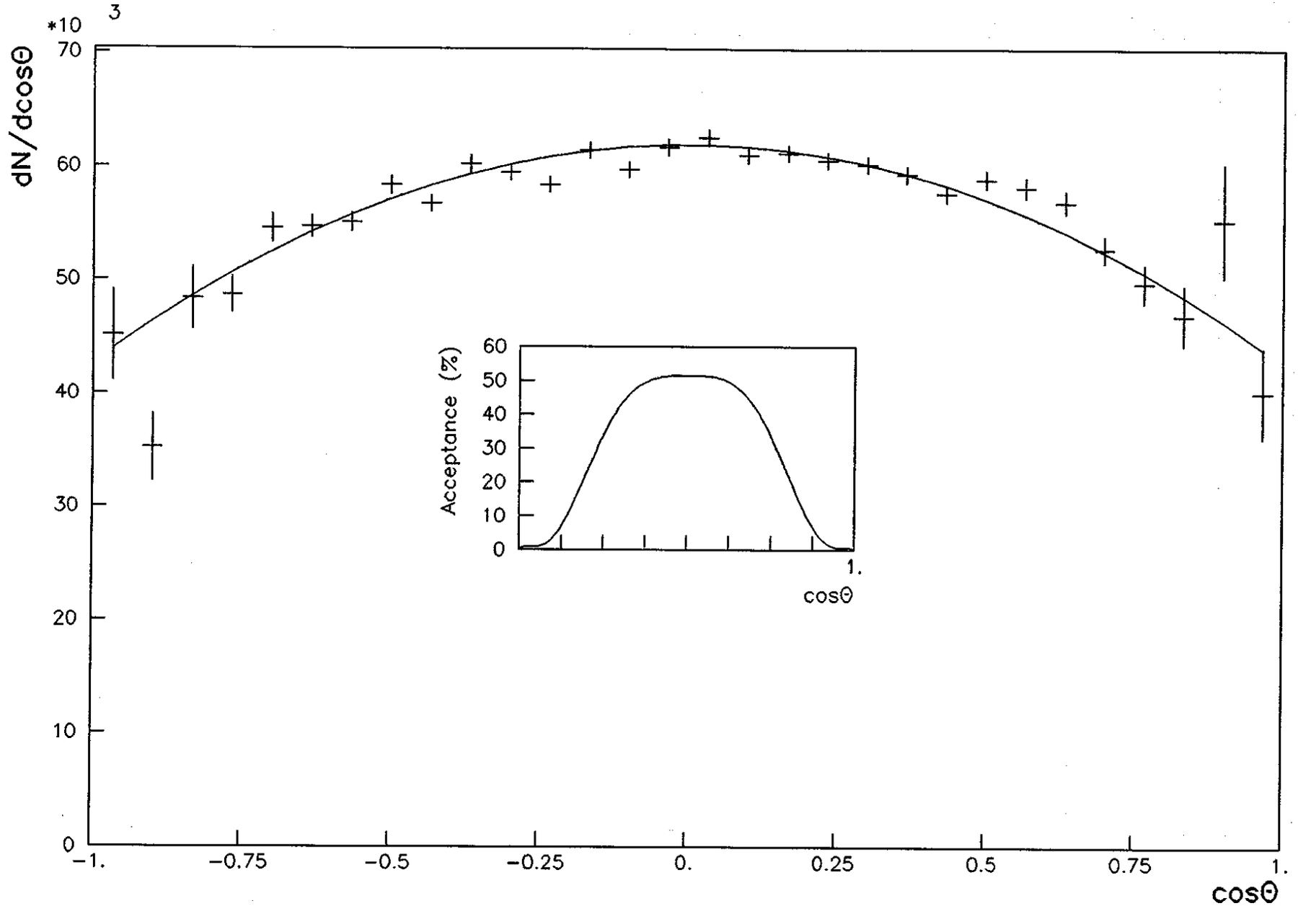
*10 3
dN/dcosΘ
70
60
50
40
30
20
10
0
−1.
−0.75
−0.5
−0.25
0.
0.25
0.5
0.75
1.
cosΘ
Acceptance (%)
60
50
40
30
20
10
0
1.
cosΘ

FIG. 14

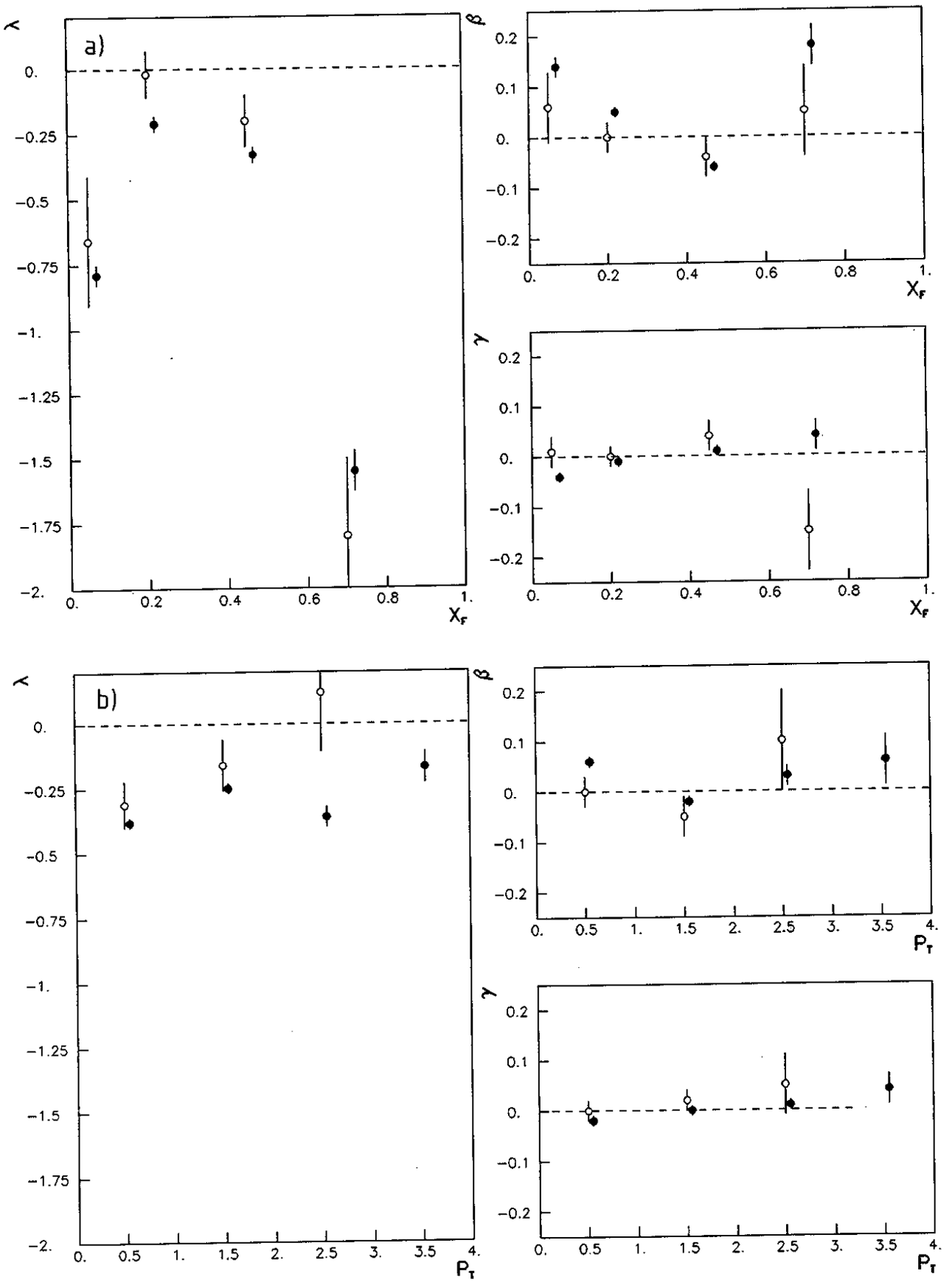

FIG. 15